HHS Public Access

Author manuscript

Neuroimage. Author manuscript; available in PMC 2015 May 21.

Published in final edited form as:

Neuroimage. 2014 March ; 88: 143–154. doi:10.1016/j.neuroimage.2013.11.025.

Diffusion properties of major white matter tracts in young, typically developing children

Ryan T. Johnson[1], **Jason D. Yeatman**[2], **Brian A. Wandell**[2], **Michael H. Buonocore**[3], **David G. Amaral**[1], and **Christine W. Nordahl**[1,*]

[1]M.I.N.D. Institute and Department of Psychiatry and Behavioral Sciences, University ofCalifornia at Davis, 2825 50th Street, Sacramento, CA 95817, USA

[2]Department of Psychology, Jordan Hall, Stanford University, 450 Serra Mall, Stanford, CA 94305, USA

[3]Department of Radiology, UC Davis School of Medicine, University of California, Sacramento, CA 95817

Abstract

Brain development occurs rapidly during the first few years of life involving region-specific changes in both gray and white matter. Due to the inherent difficulties in acquiring magnetic resonance imaging data in young children, little is known about the properties of white matter in typically developing toddlers. In the context of an ongoing study of young children with autism spectrum disorder, we collected diffusion-weighted imaging data during natural nocturnal sleep in a sample of young (mean age = 35 months) typically developing male and female (n = 41 and 25, respectively) children. Axial diffusivity, radial diffusivity, mean diffusivity and fractional anisotropy were measured at 99 points along the length of 18 major brain tracts. Influences of hemisphere, age, sex, and handedness were examined. We find that diffusion properties vary significantly along the length of the majority of tracks. We also identify hemispheric and sex differences in diffusion properties in several tracts. Finally, we find the relationship between age and diffusion parameters changes along the tract length illustrating variability in age-related white-matter development at the tract level.

Keywords

children; white matter; tractography; development; sex differences; laterality

[*]Corresponding Author: Christine Wu Nordahl, PhD, Assistant Professor, Department of Psychiatry and Behavioral Sciences, University of California Davis MIND Institute, Sacramento, CA 95820, (916) 703-0373, crswu@ucdavis.edu.

1 Introduction

Early in life the human brain develops quickly. For example, brain volume expands from approximately 25% of adult size at birth to 75% by 2 years of age and 95% by 6 years of age (Knickmeyer et al., 2008; Pfefferbaum et al., 1994). MRI in children and adolescents has revealed rapid growth in both gray and white matter but with considerable regional variability (Huang et al. 2006; Huttenlocher et al. 1997; Jernigan et al. 1991; Peterson et al. 2003; Gilmore et al. 2007, 2012; Giedd et al. 1996; Nordahl et al. 2012; Toga et al. 2006). Multiple factors such as age, sex and hemispheric asymmetry likely contribute to this variability in brain growth (Bonekamp et al. 2007; Eluvathingal et al. 2007; Giedd et al. 1997; Lebel & Beaulieu 2009; Paus et al. 1999; Schmithorst et al. 2008; Trivedi et al. 2009). Accounting for these factors will produce a more thorough understanding of typical early brain development, which is critical for advancing research in neurodevelopmental disorders (Honea et al., 2005; Gabrieli, 2009; Qiu et al., 2008; Thiebaut de Schotten et al. 2011; Yeatman et al., 2012a).

The inherent difficulties in acquiring magnetic resonance imaging (MRI) data from young children means that relatively little information has been gathered regarding typical brain development prior to 5 years of age. Diffusion-tensor imaging (DTI) allows for detailed exploration of pediatric brain anatomy and has provided important information regarding white-matter development. While most major white matter tracts can be identified at birth, examination of tracts in young children has been somewhat lacking with rare exceptions (Duboise et al. 2006; Huang et al., 2006; Hermoye et al., 2006; Qiu et al. 2013; Trivedi et al., 2009; Weinstein et al., 2010; Wolff et al., 2012; Yap et al. 2011).

White matter tracts consist of thousands of axons entering and exiting at various points to reach specific targets. Thus, using a single diffusion parameter to characterize the entirety of a tract may mask potentially valuable information. To account for this variability and provide a detailed characterization of white matter tract structure during early childhood, we used newly available tractography software (Yeatman et al., 2012b) to analyze 18 white matter tracts in typically developing male and female toddlers ranging in age from 26 to 46 months. We quantified diffusion parameters along the length of each tract and identified localized differences while comparing tract properties between hemispheres and in relation to the age and gender of the subjects. We found substantial within-tract variability in many tracts as well as location specific sexual dimorphisms and differential effects of age on tract diffusion properties.

2 Materials and Methods

2.1 Participants

Participants were recruited through the M.I.N.D (Medical Investigation of Neurodevelopmental Disorders) Institute of the University of California, Davis (UCD), as part of the Autism Phenome Project. Diffusion imaging data were acquired from typically developing children including 41 males and 25 females (Table 1). Participants were recruited as part of a study on autism spectrum disorder, though children with ASD were not included in the present study. Inclusion criteria for the typically developing children included scores

within ± 1.5 standard deviations of the mean on all subscales of the Mullens Scales of Early Development. Handedness was assessed by means of behavioral examination. Exclusion criteria were physical contraindications to MRI, diagnosis with a pervasive developmental disorder, specific language impairment or any known developmental, neurological, or behavioral problems. All children were native English speakers. The UCD institutional review board approved this study, and informed consent was obtained from the parent or guardian of each participant.

2.2 Imaging Procedures

MRI scans were acquired during natural nocturnal sleep at the UC Davis Imaging Research Center using a 3T Siemens Trio whole-body MRI system (Siemens Healthcare, Inc., Erlangen, Germany) equipped with an 8-channel head coil (Invivo, Inc., Gainesville, Fl). The scanner room was decorated to be child-friendly with colorful wall hangings, pillows and stuffed animals. Earplugs and/or headphones were used to attenuate scanner noise and children were closely monitored during scanning. This approach has proven highly successful with a success rate of over 85% (Nordahl et al., 2008).

For all participants, images were obtained using a three-dimensional T1-weighted MPRAGE sequence (TR 2170 ms; TE 4.86 ms; matrix 256 x 256; 192 slices in the sagittal direction, 1.0 mm isotropic voxels, scan time: 8 m 6 s) and a diffusion-weighted, spin echo, echo planar imaging sequence (“ep2d_diff”, number of slices: 72, slice thickness: 1.9 mm, slice gap: 0.0, matrix size: 128x128, voxel size: 1.9 mm isotropic, phase encoding direction: anterior to posterior (A≫P), phase partial Fourier: 5/8, TR: 11500, TE: 91, scan time: 6 m 56 s), with effective b-value 700 mm^2/s, 30 gradient directions, and five b =0 images acquired at equally spaced intervals over the scan time. T2-weighted images were also obtained for clinical evaluation when possible (i.e. when the child remained asleep). All MPRAGE and available T2 scans were reviewed by a pediatric neuroradiologist and screened for significant, unexpected clinical findings.

Images were acquired from October 2007 to June 2011. In August 2009, the Siemens 3T Trio MRI system was upgraded to a Trio Total Imaging Matrix (TIM) MRI System running version VB15A operating system software. All the VA25A sequences were upgraded and mapped to their corresponding VB15A sequences with no parameter changes having an effect on image quality or appearance, except for the diffusion-weighted sequence. For this sequence, the spatial resolution, b-value, and diffusion gradient directions were preserved, but parameters were changed to reduce the geometric distortion of the images, and the impact of the geometric distortion on the image analysis. Specifically, the phase encoding direction was changed from ‘anterior to posterior’ (A≫P) to ‘posterior to anterior’ (P≫A), to eliminate tissue compression in the anterior temporal and frontal lobes, and the iPAT option (GRAPPA) was used with a factor 2 acceleration to permit shorter TE and reduced effective echo spacing for reduced geometric distortion at all voxels. The phase partial Fourier factor was increased from 5/8 to 6/8 to partially compensate for the factor 2 reduction in data acquired using GRAPPA. The use of GRAPPA allowed TE to be reduced from 91ms to 81ms, and echo spacing to be reduced from 0.83 ms to 0.69 ms. It also allowed TR to be reduced from 11500ms to 8500ms, and scan time from 6 m 56 s to 5 m 23

s. Although the diffusion gradient parameters (directions and b-value) were not changed, the reduction in geometric distortion caused averaging (over the local tissue to determine each voxel value) to be different in the pre-upgrade versus post-upgrade images. Thus, there are likely to be differences in the diffusion parameters in regions with reduced geometric distortion. To control for these differences, we included MRI system upgrade status (pre-upgrade, post-upgrade) as a nuisance covariate for all statistical analyses involving diffusion parameters. In the current study, 29 scans (10 females, 20 males) were acquired before the scanner upgrade and 37 scans were acquired (15 females, 22 males) afterwards (Fisher's exact test, $p = 0.62$).

2.3 Image Processing and Diffusion Tensor Calculation

T1-weighted structural image preprocessing follows Nordahl et al. (2011) and included removal of nonbrain tissue using the Oxford Center for Functional MRI of the Brain (FMRIB) brain extraction tool (BET; Smith, 2002) and correction of main field (B0) inhomogeneities using the nonparametric nonuniform-intensity normalization method (N3; Sled et al., 1998). DTI data were processed using the Vistalab (Stanford Vision and Imaging Science and Technology) diffusion MRI software suite. The raw DTI dicom images were converted to 4-D nifti format and volumes and motion artifacts were excluded. DTI images were aligned to the motion-corrected mean of the non-diffusion weighted ($b = 0$) images using a rigid body algorithm. DTI images were then resampled to 2-mm isotropic voxels with eddy-current and motion correction using a 7th-order b-spline algorithm based on SPM5. Vistalab image processing software is available as part of the open-source mrDiffusion package available at http://white.stanford.edu/software/.

Diffusion tensors were fitted to the resampled DTI data using a least squares fit and the RESTORE algorithm that also removed outliers from the tensor estimation (Chang et al., 2005). The diffusion tensor model produces measures describing the diffusion characteristics of each voxel. Eigenvalues ($\lambda1$, $\lambda2$, $\lambda3$) from the diffusion tensor are used to compute axial diffusivity ($\lambda1$), radial diffusivity ($\lambda2+\lambda3/2$), mean diffusivity ($\lambda1+\lambda2+\lambda3/3$) and fractional anisotropy ($\sqrt{(1/2)}\sqrt{((\lambda1-\lambda2)^2+(\lambda2-\lambda2)^2+(\lambda3-\lambda1)^2)}/\sqrt{(\lambda1^2+\lambda2^2+\lambda3^2)}$) (Pierpaoli and Basser, 1996). Axial diffusivity (AD) describes diffusion parallel to the principle diffusion direction (i.e. along the long axis of a fascicle of fibers) and has been related to changes in axon integrity such as during axonal degeneration (Kim et al., 2007; Song et al., 2003; Sun et al., 2006; Thomalla et al., 2004). Radial diffusivity (RD) describes diffusion perpendicular to the principle diffusion direction and is decreased with reduced axonal myelination or axon tract density (Song et al., 2003; 2002; Tyszka et al., 2006; Zhang et al., 2009). Mean diffusivity (MD) and fractional anisotropy (FA) are summative measures that describe average total diffusion and a normalized standard deviation of the three diffusion directions, respectively.

2.4 Automatic Fiber Quantification

We used Automatic Fiber Quantification (AFQ) software tools to identify 18 white matter tracts in each participant's brain. AFQ and consists primarily of steps: (1) whole-brain tract tractography (2) ROI-based tract segmentation and cleaning (3) quantification. After ROI-based segmentation, fiber tracts were cleaned using a statistical outlier rejection algorithm.

First each fiber in a fiber group is sampled to 99 equidistant nodes. Then the spread of fibers at each node is represented as a 3 dimensional gaussian distribution and any fiber that is more than 5 standard deviation from the core (mean) of the tract is removed. The procedure is repeated until there are no more fiber outliers. Diffusion properties are then calculated along the trajectory of the fiber group by interpolating the image value (FA, MD, AD, RD) at each node along each fiber. Tract Profiles of each parameter are then calculated as a weighted sum of each fiber's value at a given node where a fiber is weighted based on its Mahalanobis distance from the core or mean location of the tract. AFQ tractography yields tracts similar to those seen in other reports in this participant age range (Figure 1, Huang et al., 2006; Trivedi et al., 2009; Wolff et al., 2012). Furthermore, tractography results generally match the overall shape and anatomical paths seen in older children and adults (Goodlett et al., 2009; Hermoye et al., 2006; Huang et al., 2006; Lebel et al., 2012). AFQ is described in greater detail in Yeatman et al. 2012b.

Because AFQ uses strict criterion for tract identification, it did not identify all 18 tracts in each participant. As might be expected, image quality was a significant determinant of AFQ's ability to segment and identify tracts, and there was greater success with scans acquired after the scanner and sequence update (see Imaging Procedures above). Details regarding tract identification rates and their influence on the total N used in analysis are shown in Table 2.

For the most part, tract identification did not differ in the left and right hemisphere. However, both the cingulum and arcuate fasciculus had greater probability of identification in the left hemisphere than in the right (left cingulum 85%, right cingulum 71%, Fisher's exact test $p < 0.05$; Left arcuate fasciculus 87%, right arcuate fasciculus 52%, Fisher's exact test $p < 0.001$). Difficulty in identifying the right arcuate fasciculus using tractography is a consequence of the right tract exhibiting higher curvature and greater partial voluming with the superior longitudinal fasciculus compared to the left arcuate fasciculus (Catani et al., 2007; Lebel and Beaulieu, 2009; Mishra et al., 2010; Yeatman et al., 2011). Laterality of cingulum diffusion parameters has been previously reported in adults (Gong et al., 2005a). The significant asymmetry in all four diffusion parameters for the cingulum likely contributed to the difference in identification rates and is discussed in more detail below.

Tract identification was also not influenced by participant sex with the exception of the right and left inferior longitudinal fascicles (ILF; Fisher's exact test, ps < 0.001). These tracts were identified less often in males than in females. Sex differences in diffusion parameters have been found in the ILF previously (Choi et al., 2010) and in the current study (see Effects of Sex below). If diffusion is lower in males through much of this tract's bundle, this may lead to a greater chance of exclusion during tractography.

2.5 Statistical Approach

For each subject, AD, RD, MD, and FA were calculated at 99 nodes between the two defining ROIs for each tract. For all differential analysis, separate three-way mixed-design analyses of co-variance (ANCOVA) were conducted for the continuous dependent variables (AD, RD, MD, FA). Hemisphere and nodes were used as repeated measures and sex as a between-group measure. For hemisphere analysis in the forceps major and minor nodes 1–

49 were compared to nodes 50–99. Participant age was included as a continuous covariate while handedness and scanner status were controlled.

Mauchly's test of sphericity (Mauchly, 1940) was used to test for violations of sphericity and the Greenhouse-Geisser correction (Greenhouse and Geisser, 1959) was applied when sphericity was violated. Follow-up one-way ANCOVAs and Bonferroni-corrected pairwise comparisons were used to further investigate significant main-effects and interactions identified in the omnibus tests. Because the repeated measure of nodes was nested within the repeated measure of hemisphere, pairwise comparisons of hemisphere mean differences (averaged across nodes) were considered useful and informative in the absence of significant omnibus hemisphere effects. For correlations between age and diffusion properties, partial correlations controlling for scanner upgrade status were used. For all analyses, results are expressed as mean ± SEM (standard error of the mean), and a p-value less than 0.05 was considered statistically significant.

3 Results

3.1 Effects of Hemisphere

For all tracts except the forceps minor, significant effects of hemisphere were seen for most of the diffusion parameters (Figure 2, Table 3). When significantly different, mean AD was generally higher in the right hemisphere, with the only exception being in the cingulum. Similarly, mean RD was usually higher in the right hemisphere. Mean MD was also higher in the right hemisphere for several tracts. Mean FA was higher in several left hemisphere tracts. It was higher in the right hemisphere only for the superior longitudinal fasciculus (SLF). Corrected comparisons between hemisphere diffusion parameter means are detailed in Table 3.

In every case in which FA was greater in one hemisphere, AD and/or RD were asymmetric as well. However, in the thalamic radiation and uncinate fasciculus, AD or RD was asymmetric without an asymmetry in FA. Due to the substantial between hemisphere variability indicated by these analyses, subsequent analyses reported below were conducted independently for each hemisphere.

3.2 Effects of Nodes

For the majority of tracts, diffusion properties varied significantly along the length of the tract (Figure 2). AD, RD and MD were significantly variable in 8, 6 and 10 tracts respectively. FA was variable in 4 tracts. Only the left inferior fronto-occipital fasciculus (IFOF), left and right inferior longitudinal fasciculus (ILF), and left and right superior longitudinal fasciculus (SLF) exhibited relative homogeneity along their length for all diffusion properties. Statistical comparisons for the effects of nodes on each tract are shown in Table 4.

3.3 Effects of Sex

Male and female participants exhibited significant differences in the diffusion parameters in 4 tracts. The most prominent sex difference was seen in the left cingulum bundle (Figure 3).

AD in the cingulum was greater in males than in females (main effect of sex: $F(1,98) = 5.71$, $p < 0.05$). Corrected comparisons revealed that the AD differences were restricted mostly to two bands of nodes along the tract length; one caudal portion of the anterior cingulate and a second larger band adjacent to the posterior cingulate. RD was higher in females than in males (main effect of sex: $F(1,98) = 5.95$, $p < 0.05$). This was restricted to one large band of nodes near the posterior cingulate. The elevated AD in males and elevated RD in females also resulted in a sex difference in FA (main effect of sex: $F(1,98) = 9,93$, $p < 0.005$) with FA being higher in males than in females in both a small band at the anterior end of the tract and a larger band at its posterior portion.

Sex differences were also found in the right IFOF (Figure 4). AD was higher in males (main effect of sex: $F(1,98) = 5.24$, $p < 0.05$). Although there was a small band of significantly different AD near the anterior portion of the IFOF, the largest band of difference was at the posterior end of the tract. Mean diffusivity was also higher in males in this location (interaction of nodes and sex: $F(1,2.38) = 2.95$, $p < 0.05$).

Additional sex differences were found in the left ILF and right uncinate fasciculus (Figure 5). FA was higher in females in the left ILF in two distinct bands towards the anterior end of the tract (main effect of sex: $F(1,98) = 7.17$, $p < 0.05$). FA was also higher in females in the right uncinate in a band near the temporal end of the tract (interaction of nodes and sex: $F(1,4.47) = 2.69$, $p < 0.05$).

Two tracts had additional interactions involving participant sex. In the cingulum, the interaction between hemisphere and sex was significant ($F(1,98) = 4.69$, $p < 0.05$) with females exhibiting less laterality than males (females: left hemisphere 0.41±0.10, right hemisphere 0.39±0.01; males: left hemisphere 0.48±0.01, right hemisphere 0.041±0.01). In the uncinate, the interaction between sex, hemisphere, and nodes was significant for RD ($F(1,5.49) = 2.97$, $p < 0.05$) and FA ($F(1,5.3) = 2.58$, $p < 0.05$). RD is lower in the right uncinate fasciculus compared to the left in the temporal portion of the tract and then becomes higher in the right uncinate compared to the left in females. In males, RD is higher in the right uncinate fasciculus compared to the left and then becomes lower compared to the left as the tract passes into the frontal lobe.

3.4 Age as a Covariate of Interest

We found age to be a significant contributor to variation in 5 tracts: the forceps minor, left IFOF, left SLF, left uncinate fasciculus, and right arcuate fasciculus. For the forceps minor, the left IFOF and the left uncinate fasciculus, age was significant as a main effect. In the left and right arcuate fasciculus, age emerged in a significant interaction with nodes. We chose to examine the correlations between age and diffusion parameters in these tracts.

Examining partial correlations at each node (scanner status and handedness controlled) revealed substantial variation in the correlation between age and diffusion parameters (Figure 6). In the forceps minor, RD, AD and MD were negatively correlated with age. However, the relationship was particularly strong near where the forceps minor passes through the genu of the corpus callosum. In the left IFOF, FA exhibited a variable but mostly positive relationship with age; the strongest correlations were near the frontal end of the

tract. AD in the left SLF was both negatively and positively correlated with age with a strong positive correlation near the frontal termination of the tract. In the left uncinate fasciculus, MD is most strongly correlated with age as the tract begins to leave the temporal lobe and passes near the IFOF. The right arcuate exhibited highly variable correlations with age along the tract length for RD, MD and FA. For each diffusion parameter in the arcuate fasciculus, correlations reversed in sign near the temporo-parietal termination point of the tract.

3.5 Participant Handedness as a Covariate

Evidence for a handedness effect on white-matter diffusion parameters in young children is limited. However, handedness effects have been revealed in adults in some tracts (Gong et al., 2005a). We included handedness as a covariate to control for potential confounding effects without specific hypotheses. Handedness emerged as a significant covariate in seven tracts for various diffusion parameters: FA in the right corticospinal tracts, MD in the left cingulum, FA, AD, MD and RD in the forceps minor, FA in the right inferior fronto-occipital IFOF, FA in the right ILF, FA in the right uncinate and RD, MD in the right arcuate. In general, FA tended to be higher and MD lower in right handed subjects compared to left handed subjects.

4 Discussion

Differences in the progression of tract diffusion parameters are thought to reflect differential rates of axonal refinement, packing and myelination as part of overall white matter maturation (Beaulieu 2002, Takahasi et al. 2000; Song et al. 2002; 2005; but see Wheeler-Kingshott et al. 2009). However, few studies have investigated the variation in diffusion parameters along the length of major fasciculi in relation to hemisphere and sex before the age of 5, a time when the brain is changing rapidly. We found diffusion parameter variability related to sex, hemisphere and age in multiple white matter tracts within a sample of 26–46 month old typically developing young children. In addition, we found that diffusion parameters vary substantially along the length of a single fiber tract.

4.1 Diffusion Parameters Vary Along Tract Length in Young Children

Previous reports have measured integrated mean diffusion parameters across the entire tract within the age range reported here (Fletcher et al., 2010; Hermoye et al. 2006; Lebel et al., 2012; Trivedi et al., 2009). However, this is the first report to describe within-tract variability at this age. The variations in diffusion at different sample positions likely reflect a combination of factors including variations in myelination, axonal density, and axonal diameter as well as the influence of tract curvature, partial voluming effects and the entrance and exit of smaller axonal bundles from the larger tract (Figure 7). Diffusion properties are effected by biological properties of the axons in a voxel (eg. myelination, axonal density and axonal diameter) as well as the geometric configuration of the axons (eg. curvature, directional coherence and crossing fiber tracts). We find that diffusion properties vary substantially along the trajectory of a fascicle. For example, in the forceps minor, AD is low as the tract terminates at various targets within the frontal lobe and rises sharply as the tract forms a cohesive bundle while crossing the midline via the genu of the corpus callosum (Figure 2). Similarly, RD is high in the thalamic radiation where the tract originates, but

drops considerably as the tract enters the dense collection of myelinated white matter in the anterior limb of the internal capsule and rises again as the tract enters the cortical gray matter. Since these measurements were made in young children it is likely that some of the variation in diffusion properties is due to variation in the amount of myelin along the tract length as well (Duboise et al. 2006). In addition, white matter contains crossing, branching and merging fiber bundles and these geometric properties will have a substantial impact on the diffusion properties of a voxel (Jones 2002). For example a bundle of axons that crosses through the main fascicle will hinder diffusion parallel to the fascicle but allow more diffusion perpendicular to the fascicle (Yeatman et al. 2012b). This will also lead to a reduction in fractional anisotropy. We believe that a portion of the variance in diffusion properties that we observe along the length of these fascicles is the product of crossing, merging and branching fibers.

The different tract profiles for AD, RD, MD and FA emphasize the importance of examining more than one diffusion parameter. For example, in the corticospinal tract, AD and RD are both elevated while the tract is within the brain stem. At this level, the corticospinal tract is mostly surrounded by transverse fibers of the pons which travel perpendicular to the corticospinal tracts. Partial voluming with these tracts likely produces the elevated RD seen at this point, which in combination with high AD, results in low FA values. AD values peak again where the corticospinal tract enters the internal capsule. However, radial diffusivity there remains low. This is likely because the corticospinal tract makes up the majority of the anterior portion of the posterior limb of the internal capsule resulting in less perpendicular diffusion. As a result, FA is highest at this point in the corticospinal tract. Patterns of variability within the four diffusion properties are informative in other tracts as well.

4.2 Sex Differences in Diffusion Parameters

We found sexual dimorphism in portions of 4 tracts: the left cingulum, the right IFOF, the left ILF, and the right uncinate. The cingulum exhibited the most dramatic sex differences with significant effects for AD (males > females), RD (females > males) and FA (males > females; Figure 3). Sexual dimorphism of cingulum diffusion parameters is seen in adults (Hsu et al., 2008; Huster et al., 2009; Rametti et al., 2011) and over lifespan development (Kochunov et al., 2012; Lebel et al., 2012; Lebel and Beaulieu, 2011; Trivedi et al., 2009). Consistent with the current data, the majority of reports find FA is higher in males (but see Schneiderman et al., 2007) and the sexual dimorphism appears most often in the left cingulum. The cingulum is involved in attention, emotion and memory, and sexual dimorphisms in regions connected to the cingulum such as the cingulate cortex and the amygdala are also common (Biver et al., 1996; Giedd et al., 1997; Gur et al., 1995; Johnson et al., 2008; Merke et al., 2003; Paus et al., 1996; Pujol et al., 2002; Wrase et al., 2003).

Sexual dimorphism was also seen in the IFOF (Figure 4). The IFOF has been linked to semantic understanding (Duffau, 2008), reading (Catani and Mesulam, 2008) and visual processing (Fox et al., 2008). Reduced mean RD in adult females has previously been reported in the right IFOF (Eluvathingal et al., 2007). Interestingly, increased FA in adult males has been reported in a voxel cluster near the location of the smaller band of sexually dimorphic AD seen in children (Figure 4; Rametti et al., 2011). While not identical to our

results, these findings suggest sex differences persist in the IFOF. Furthermore, the large posterior band of sex differences approximates the point where the IFOF sharply radiates to eventual terminations in parietal, occipital and posterior temporal cortices. There are sexual dimorphisms in cortical thickness (females > males) in the right inferior parietal and posterior temporal regions (Sowell et al., 2007), which may be related to sexual dimorphism in this tract.

We also found a sex difference in FA within the left ILF (Figure 5). The ILF consists of long and short tracts with the more lateral short tracts connecting adjacent nonpolar temporal gyri. The sex differences in FA may be due to differing amounts of short tracts entering or exiting the tract near the two bands of significant differences. Overall RD and MD are lower in the ILF of adolescent females compared to males (Eluvathingal et al., 2007), and two previous lifespan reports also found sex differences in ILF FA with the same (Hasan et al., 2010) and opposite (Lebel et al., 2012) direction as the current data (male FA > female). Face recognition and emotional memory which are associated with the ILF and it's connected regions (Fox et al., 2008; Philippi et al., 2009) also sexually dimorphic with women outperforming men on face recognition and emotional memory tasks (Cahill et al., 1996; Cellerino et al. 2004; Lewin and Herlitz 2002).

The right uncinate fasciculus was sexually dimorphic as well (Figure 5). Two other lifespan studies starting at 5 years found higher mean FA in the uncinate fasciculus of males compared to females suggesting this sex difference is persistent (Lebel et al., 2012; Lebel and Beaulieu, 2011). Like the SLF and cingulum, the uncinate connects polar temporal lobe areas, including the amygdala, to cortical regions. Interestingly, a study examining 12-year-old male and female children born preterm found a group by sex interaction using ROI analysis of the right uncinate fasciculus. In control participants, males had higher FA compared to females, but in the preterm group, males had lower FA. Verbal IQ and Peabody Picture Vocabulary Test-Revised scores were correlated with both right and left uncinate fasciculus scores in the preterm male group (Constable et al., 2008).

These findings demonstrate multiple fiber tract diffusion parameter sexual dimorphisms are present in young children. The overall pattern of tract differences suggest sexual dimorphism in connections between visual and emotion/memory centers (ILF), visual and higher-order processing centers (IFOF), emotion/memory centers and higher-order processing centers (uncinate, cingulum). Most of the cortical and sub-cortical targets of these tracts are sexually dimorphic in adults and exhibit high levels of steroid hormone receptor concentration in animal models (see Goldstein et al. 2001). We suspect these tract sexual dimorphisms are the result of organizational actions of steroid hormones or sex chromosome genetics occurring in utero or during the perinatal hormone surge.

In addition, these sex differences are concentrated in select locations along the tracts. One possible explanation is that hormone sensitive gray matter regions produce sexually dimorphic axonal contributions to these tracts which manifest in diffusion parameter differences at these locations. Alternately, diffusion parameter sexual dimorphisms may be due to greater tract curvature or partial voluming with adjacent structures or even different rates of tract myelination. Sexual differentiation studies incorporating localized measures of

diffusion in both younger and older children will produce a map of white matter sexual dimorphism emergence, which may be useful in understanding disorders with sex biases in the population.

4.3 Age Effects in Diffusion Parameters

Age is known to be an important factor in measures of white matter diffusion. The few neonatal DTI studies available show considerable change in fiber tract diffusion parameters during neonatal life, but the rate of change appears to slow past 24 months (Hermoye et al., 2006; Huang et al., 2006; Trivedi et al., 2009). Lifespan development studies starting from age 5 describe increases in FA followed by a plateau for most tracts during early adulthood and a slow decline during old age with an opposite pattern for MD (Eluvathingal et al., 2007; Lebel et al., 2012; Lebel and Beaulieu, 2011; Lebel et al., 2008; Schmithorst, 2009). Similar to results in older children, we found generally positive relationships between age and FA (Figure 6; left IFOF, right arcuate) and mostly negative relationships between age and MD (Figure 6; forceps minor, left uncinate).

Increasing FA with age is thought to be driven by decreasing RD as white matter become increasingly myelinated (Bonekamp et al., 2007; Eluvathingal et al., 2007; Hasan et al., 2010; Verhoeven et al., 2009; Westlye et al., 2010). This was the case in the right arcuate where RD and FA displayed opposing correlations with age. In the left IFOF, the only other tract to show a significant age effect for FA, the effect of age on RD approached significance for RD ($p = 0.069$).

The current data help bridge the age gap in our understanding of white matter in children and provide additional details in several tracts by illustrating that aging does not uniformly influence tract diffusion parameters. We suspect other tracts undergo similar age-related changes along their length but the restricted age range in our participants, spanning 26–46 months, reduced the number of age effects in the omnibus tests. Longitudinal analysis using AFQ will clarify patterns in tract maturation with a new level of detail.

4.4 Laterality in Diffusion Parameters

Similar to sexual dimorphism, asymmetry in white-matter diffusion parameters is region specific and age-dependent (Ardekani et al., 2007; Bonekamp et al., 2007; Hasan et al., 2010; Liu et al. 2010; Trivedi et al., 2009). Studies in very young children suggest left-ward asymmetries with higher fractional anisotropy in the left corticospinal tract, left superior longitudinal fasciculus, left arcuate fasciculus and possibly the left thalamic radiations (Dubois et al. 2009; Liu et al. 2010). Lifespan development reports (mostly starting above age 5) also suggest a mild leftward asymmetry in overall FA but with few significant comparisons among specific tracts (Lebel et al., 2012; Trivedi et al., 2009). We found diffusion parameter asymmetries in 9 of the 10 tract pairs/sides examined (Figure 2, Table 3). Several of these asymmetries have been reported in adults (Bonekamp et al., 2007; Büchel et al., 2004; Thiebaut de Schotten et al., 2011; Westerhausen et al., 2007) and leftward asymmetries in the arcuate fasciculus and cingulum are especially prevalent.

Mean FA and tract density are greater in the left arcuate fasciculus compared to the right in adults and older children (Büchel et al., 2004; Dubois et al. 2009; Fletcher et al., 2010; Lebel

and Beaulieu, 2009; Paus et al., 1999; Powell et al., 2006; Rodrigo et al., 2007). We also observed asymmetry of arcuate FA in younger children (Figure 2). In agreement with Fletcher et al.'s (2010) description in typically developing adolescent boys, we also found higher MD and RD in the right arcuate compared to the left (Table 3). Asymmetry in the arcuate fasciculi is linked to faster maturation in the left arcuate due to the important role it plays in that hemisphere's language circuit (Klingberg et al., 2000; Rauschecker et al., 2009; Rolheiser et al., 2011; Yeatman et al., 2011).

A second consistent asymmetry is a leftward bias in cingulum FA which is robust and present over the lifespan (Bonekamp et al., 2007; Gong et al., 2005a; 2005b; Trivedi et al., 2009; Wilde et al., 2009). We confirmed higher mean FA in the left cingulum of children and show that this is the product of higher AD in the left cingulum and higher RD in the right cingulum (Figure 2). The greater AD in the left and greater RD in the right cingulum suggest a more cohesive tract bundle with possibly greater axonal density and myelination in the left hemisphere.

Several of the cingulum's gray matter targets such as the cingulate cortex and amygdala also exhibit considerable laterality (Huster et al., 2007; Paus et al., 1996; Yücel et al., 2001; Andersen and Teicher, 1999; Cooke et al., 2007; Gasbarri et al., 2007; Giedd et al., 1997; Johnson et al., 2008; Killgore et al., 2001; Scicli et al., 2004), and laterality in anterior cingulate gray matter has been linked to personality, executive-control, and risk for psychotic illness (Fornito et al., 2004; Pujol et al., 2002; Yücel et al., 2003). The current data illustrate that the cingulum, which receives contributions from both the amygdala and cingulate cortex, is also asymmetric from a young age in humans.

5 Limitations

The current study provides a new level of detail regarding white matter diffusion parameters in young children, but there are a few issues to note. Although AFQ provides a method to assess within tract variance, the use of a tensor models means we do not trace the trajectory of fiber tracts crossing the principle tract bundle in a voxel. This means we measure the core of a tract but do not measure all of its smaller branches. Relatedly, diffusion parameters were not measured at the extremes of each tract near the cortical endpoints. Measuring in these areas may provide useful information but will likely also be subject to extremely high levels of variability due to partial voluming with gray matter. Additionally, because AFQ tracts fibers in native space, due to individual variability in factors such as tract curvature, tract size, and image quality, some tracts entered statistical analysis with a greater sample size than others (Table 2). Additional analysis of the right cingulum and right arcuate, the only tracts with fewer than 50 subjects, might identify additional within or between subjects effects in these tracts. Finally, because the current data are part of a larger longitudinal study taking place over several years, improvements to the research center's scanner software occurred during data collection. To account for this, we have included scanner status as a covariate in our analyses. While there were differences in fiber identification rates (Table 2) the between-subjects factor in our model (participant sex) was not differentially distributed among the two scanner statuses (Fisher's exact test, $p = 0.62$).

6 Conclusions

Our results indicate that in young children, factors such as within-tract variability, sex, hemisphere and age, exhibit variable influence on diffusion parameters along the major fasciculi. These findings also illustrate how repeated sampling of multiple diffusion parameters produces a more detailed understanding of a tract than mean measures of a single descriptor such as fractional anisotropy or mean diffusivity. Normal variation in tract diffusion parameters can be caused by gross properties such as tract curvature and partial voluming with nearby structures but may also illustrate changes in local myelination, axonal density and/or the addition and elimination of axons to the tract. Given the highly variable patterns of correlation between age and diffusion parameters along the tract length, longitudinal studies describing changes to the diffusion parameter profile of a tract are particularly informative.

The present study provides an enhanced level of detail regarding sexual dimorphism and hemispheric asymmetry in tract diffusion properties. Abnormal cerebral asymmetry has been linked to intellectual deficits and schizophrenia (Burns et al., 2003; Crow, 2004; Rosenberger and Hier, 1980; Wang et al., 2004) and disorders such as autism and depression exhibit pronounced sex biases in the population. A more thorough understanding of how sexual dimorphism and hemispheric asymmetry influence major fasciculi in normative development may improve our ability to identify white matter abnormalities in several disorders.

Acknowledgments

The authors would like to thank Shae DiNino, Kayla Harrington, Aaron Lee, Deana Li, Sarah Liston and Mark Shen for technical assistance in data collection and processing. We also thank Sally Rogers, Sally Ozonoff and Lesley Deprey for collection and assistance in interpreting handedness data, all of the APP staff involved in the logistics of the study, and all the families who participated in the Autism Phenome Project.

References

Andersen SL, Teicher MH. Serotonin laterality in amygdala predicts performance in the elevated plus maze in rats. Neuroreport. 1999; 10:3497. [PubMed: 10619632]

Ardekani S, Kumar A, Bartzokis G, Sinha U. Exploratory voxel-based analysis of diffusion indices and hemispheric asymmetry in normal aging. Magn Reson Imaging. 2007; 25:154–167. [PubMed: 17275609]

Beaulieu C. The basis of anisotropic water diffusion in the nervous system - a technical review. NMR Biomed. 2002; 15:435–455. [PubMed: 12489094]

Biver F, Lotstra F, Monclus M, Wikler D, Damhaut P, Mendlewicz J, Goldman S. Sex difference in 5HT2 receptor in the living human brain. Neurosci Lett. 1996; 204:25–28. [PubMed: 8929969]

Bonekamp D, Nagae LM, Degaonkar M, Matson M, Abdalla WMA, Barker PB, Mori S, Horská A. Diffusion tensor imaging in children and adolescents: reproducibility, hemispheric, and age-related differences. Neuroimage. 2007; 34:733–742. [PubMed: 17092743]

Büchel C, Raedler T, Sommer M, Sach M, Weiller C, Koch MA. White matter asymmetry in the human brain: a diffusion tensor MRI study. Cereb Cortex. 2004; 14:945–951. [PubMed: 15115737]

Burns J, Job D, Bastin ME, Whalley H, Macgillivray T, Johnstone EC, Lawrie SM. Structural disconnectivity in schizophrenia: a diffusion tensor magnetic resonance imaging study. Br J Psychiatry. 2003; 182:439–443. [PubMed: 12724248]

Cahill LF, Haier R, Fallon J. Amygdala activity at encoding correlated with long-term, free recall of emotional information. Proc Natl Acad Sci USA. 1996; 93:8016–8021. [PubMed: 8755595]

Catani M, Allin MPG, Husain M, Pugliese L, Mesulam MM, Murray RM, Jones DK. Symmetries in human brain language pathways correlate with verbal recall. Proc Natl Acad Sci USA. 2007; 104:17163–17168. [PubMed: 17939998]

Catani M, Mesulam M. The arcuate fasciculus and the disconnection theme in language and aphasia: history and current state. Cortex. 2008; 44:953–961. [PubMed: 18614162]

Chang L-C, Jones DK, Pierpaoli C. RESTORE: robust estimation of tensors by outlier rejection. Magn Reson Med. 2005; 53:1088–1095. [PubMed: 15844157]

Cellerino A, Borghetti D, Sartucci F. Sex differences in face gender recognition in humans. Brain Res Bull. 2004; 63:443–449. [PubMed: 15249109]

Choi CH, Lee JM, Koo BB, Park JS, Kim DS, Kwon JS, Kim IY. Sex differences in the temporal lobe white matter and the corpus callosum: a diffusion tensor tractography study. Neuroreport. 2010; 21:73–77. [PubMed: 19996809]

Constable RT, Ment LR, Vohr BR, Kesler SR, Fulbright RK, Lacadie C, Delancy S, Katz KH, Schneider KC, Schafer RJ, Makuch RW, Reiss AR. Prematurely Born Children Demonstrate White Matter Microstructural Differences at 12 Years of Age, Relative to Term Control Subjects: An Investigation of Group and Gender Effects. Pediatrics. 2008; 121:306–316. [PubMed: 18245422]

Cooke BM, Stokas MR, Woolley CS. Morphological sex differences and laterality in the prepubertal medial amygdala. J Comp Neurol. 2007; 501:904–915. [PubMed: 17311322]

Crow TJ. Cerebral asymmetry and the lateralization of language: core deficits in schizophrenia as pointers to the gene. Current Opinion in Psychiatry. 2004; 17:97.

Dubois J, Hertz-Pannier L, Dehaene-Lambertz G. Assessment of the early organization and maturation of infants' cerebral white matter fiber bundles: a feasibility study using quantitative diffusion tensor imaging and tractography. Neuroimage. 2006; 30:1121–1132. [PubMed: 16413790]

Dubois J, Hertz-Pannier L, Cachia A, Mangin JF, Le Bihan D, Dehaene-Lambertz G. Structural Asymmetries in the Infant Language and Sensori-Motor Networks. Cereb Cortex. 2009; 19:414–423. [PubMed: 18562332]

Duffau H. The anatomo-functional connectivity of language revisited. Neuropsychologia. 2008; 46:927–934. [PubMed: 18093622]

Eluvathingal TJ, Hasan KM, Kramer L, Fletcher JM, Ewing-Cobbs L. Quantitative diffusion tensor tractography of association and projection fibers in normally developing children and adolescents. Cereb Cortex. 2007; 17:2760–2768. [PubMed: 17307759]

Fletcher PT, Whitaker RT, Tao R, DuBray MB, Froehlich A, Ravichandran C, Alexander AL, Bigler ED, Lange N, Lainhart JE. Microstructural connectivity of the arcuate fasciculus in adolescents with high-functioning autism. Neuroimage. 2010; 51:1117–1125. [PubMed: 20132894]

Fornito A, Yücel M, Wood S, Stuart GW, Buchanan JA, Proffitt T, Anderson V, Velakoulis D, Pantelis C. Individual differences in anterior cingulate/paracingulate morphology are related to executive functions in healthy males. Cereb Cortex. 2004; 14:424–431. [PubMed: 15028646]

Fox CJ, Iaria G, Barton JJS. Disconnection in prosopagnosia and face processing. Cortex. 2008; 44:996–1009. [PubMed: 18597749]

Hermoye L, Saint-Martin C, Cosnard G, Lee SK, Kim J, Nassogne MC, Menten R, Clapuyt P, Donohue PK, Hua K, Wakana S, Jiang H, van Zijl PCM, Mori S. Pediatric diffusion tensor imaging: Normal database and observation of the white matter maturation in early childhood. Neuroimage. 2006; 29:493–504. [PubMed: 16194615]

Gabrieli JDE. Dyslexia: A New Synergy Between Education and Cognitive Neuroscience. Science. 2009; 325:280–283. [PubMed: 19608907]

Gasbarri A, Arnone B, Pompili A, Pacitti F, Pacitti C, Cahill LF. Sex-related hemispheric lateralization of electrical potentials evoked by arousing negative stimuli. Brain Res. 2007; 1138:178–186. [PubMed: 17274960]

Giedd JN, Castellanos FX, Rajapakse JC, Vaituzis AC, Rapoport JL. Sexual dimorphism of the developing human brain. Prog Neuropsychopharmacol Biol Psychiatry. 1997; 21:1185–1201. [PubMed: 9460086]

Giedd JN, Snell JW, Lange N, Rajapakse JC, Casey BJ, Kozuch PL, Vaituzis AC, Vauss YC, Hamburger SD, Kaysen D, Rapoport JL. Quantitative Magnetic Resonance Imaging of Human Brain Development: Ages 4–18. Cereb Cortex. 1996; 6:551–559. [PubMed: 8670681]

Gilmore JH, Lin W, Prastawa M. Regional Gray Matter Growth, Sexual Dimorphism, and Cerebral Asymmetry in the Neonatal Brain. J Neurosci. 2007; 27:1255–1260. [PubMed: 17287499]

Gilmore JH, Shi F, Woolson SL, Knickmeyer RC, Short SJ, Lin W, Zhu H, Hamer RM, Styner M, Shen D. Longitudinal development of cortical and subcortical gray matter from birth to 2 years. Cerebral Cortex. 2012; 22:2478–2485. [PubMed: 22109543]

Goldstein JM, Seidman LJ, Horton NJ, Makris N, Kennedy DN, Caviness VS Jr, Faraone SV, Tsuang MT. Normal sexual dimorphism of the adult human brain assessed by in vivo magnetic resonance imaging. Cereb Cortex. 2001; 11:490–497. [PubMed: 11375910]

Gong G, Jiang T, Zhu C, Zang Y, He Y, Xie S, Xiao J. Side and handedness effects on the cingulum from diffusion tensor imaging. Neuroreport. 2005a; 16:1701. [PubMed: 16189481]

Gong G, Jiang T, Zhu C, Zang Y, Wang F, Xie S, Xiao J, Guo X. Asymmetry analysis of cingulum based on scale-invariant parameterization by diffusion tensor imaging. Hum Brain Mapp. 2005b; 24:92–98. [PubMed: 15455461]

Goodlett CB, Fletcher PT, Gilmore JH, Gerig G. Group analysis of DTI fiber tract statistics with application to neurodevelopment. Neuroimage. 2009; 45:S133–S142. [PubMed: 19059345]

Greenhouse SW, Geisser S. On methods in the analysis of profile data. Psychometrika. 1959; 24:95–112.

Gur RC, Mozley LH, Mozley PD, Resnick SM, Karp JS, Alavi A, Arnold SE, Gur RE. Sex differences in regional cerebral glucose metabolism during a resting state. Science. 1995; 267:528–531. [PubMed: 7824953]

Hasan KM, Kamali A, Abid H, Kramer LA, Fletcher JM, Ewing-Cobbs L. Quantification of the spatiotemporal microstructural organization of the human brain association, projection and commissural pathways across the lifespan using diffusion tensor tractography. Brain Struct Funct. 2010; 214:361–373. [PubMed: 20127357]

Hermoye L, Saint-Martin C, Cosnard G, Lee SK, Kim J, Nassogne MC, Menten R, Clapuyt P, Donohue PK, Hua K, Wakana S, Jiang H, van Zijl PCM, Mori S. Pediatric diffusion tensor imaging: Normal database and observation of the white matter maturation in early childhood. Neuroimage. 2006; 29:493–504. [PubMed: 16194615]

Honea R, Crow TJ, Passingham D, Mackay CE. Regional deficits in brain volume in schizophrenia: a meta-analysis of voxel-based morphometry studies. Am J Psychiatry. 2005; 162:2233–2245. [PubMed: 16330585]

Hsu JL, Leemans A, Bai CH, Lee CH, Tsai YF, Chiu HC, Chen WH. Gender differences and age-related white matter changes of the human brain: A diffusion tensor imaging study. Neuroimage. 2008; 39:566–577. [PubMed: 17951075]

Huang H, Zhang J, Wakana S, Zhang W, Ren T, Richards LJ, Yarowsky P, Donohue PK, Graham E, van Zijl PCM, Mori S. White and gray matter development in human fetal, newborn and pediatric brains. Neuroimage. 2006; 33:27–38. [PubMed: 16905335]

Huster RJ, Westerhausen R, Kreuder F, Schweiger E, Wittling W. Hemispheric and gender related differences in the midcingulum bundle: a DTI study. Hum Brain Mapp. 2009; 30:383–391. [PubMed: 18064584]

Huster RJ, Westerhausen R, Kreuder F, Schweiger E, Wittling W. Morphologic asymmetry of the human anterior cingulate cortex. Neuroimage. 2007; 34:888–895. [PubMed: 17161625]

Huttenlocher PR, Dabholkar AS. Regional differences in synaptogenesis in human cerebral cortex. J Comp Neurol. 1997; 387:167–178. [PubMed: 9336221]

Jernigan TL, Hesselink JR, Sowell E, Tallal PA. Cerebral structure on magnetic resonance imaging in language- and learning-impaired children. Archives of Neurology. 1991; 48:539–545. [PubMed: 2021369]

Johnson R, Breedlove SM, Jordan CL. Sex differences and laterality in astrocyte number and complexity in the adult rat medial amygdala. J Comp Neurol. 2008; 511:599–609. [PubMed: 18853427]

Jones DK. Determining and visualizing uncertainty in estimates of fiber orientation from diffusion tensor MRI. Magn Reson Med. 2002; 49:7–12. [PubMed: 12509814]

Killgore WD, Oki M, Yurgelun-Todd DA. Sex-specific developmental changes in amygdala responses to affective faces. Neuroreport. 2001; 12:427–433. [PubMed: 11209962]

Kim JH, Loy DN, Liang HF, Trinkaus K, Schmidt RE, Song SK. Noninvasive diffusion tensor imaging of evolving white matter pathology in a mouse model of acute spinal cord injury. Magn Reson Med. 2007; 58:253–260. [PubMed: 17654597]

Klingberg T, Hedehus M, Temple E, Salz T, Gabrieli JD, Moseley ME, Poldrack RA. Microstructure of temporo-parietal white matter as a basis for reading ability: evidence from diffusion tensor magnetic resonance imaging. Neuron. 2000; 25:493–500. [PubMed: 10719902]

Knickmeyer RC, Gouttard S, Kang C, Evans D, Wilber K, Smith JK, Hamer RM, Lin W, Gerig G, Gilmore JH. A structural MRI study of human brain development from birth to 2 years. J Neurosci. 2008; 28:12176–12182. [PubMed: 19020011]

Kochunov P, Williamson DE, Lancaster J, Fox P, Cornell J, Blangero J, Glahn DC. Fractional anisotropy of water diffusion in cerebral white matter across the lifespan. Neurobiology of Aging. 2012; 33:9–20. [PubMed: 20122755]

Lebel C, Beaulieu C. Lateralization of the arcuate fasciculus from childhood to adulthood and its relation to cognitive abilities in children. Hum Brain Mapp. 2009; 30:3563–3573. [PubMed: 19365801]

Lebel C, Beaulieu C. Longitudinal development of human brain wiring continues from childhood into adulthood. J Neurosci. 2011; 31:10937–10947. [PubMed: 21795544]

Lebel C, Gee M, Camicioli R, Wieler M, Martin W, Beaulieu C. Diffusion tensor imaging of white matter tract evolution over the lifespan. Neuroimage. 2012; 60:340–352. [PubMed: 22178809]

Lebel C, Walker L, Leemans A, Phillips L, Beaulieu C. Microstructural maturation of the human brain from childhood to adulthood. Neuroimage. 2008; 40:1044–1055. [PubMed: 18295509]

Lewin C, Herlitz A. Sex differences in face recognition—Women's faces make the difference. Brain Cogn. 2002; 50:121–128. [PubMed: 12372357]

Liu Y, Balériaux D, Kavec M, Metens T, Absil J, Denolin V, Pardou A, Avni F, Van Bogaert P, Aeby A. Structural asymmetries in motor and language networks in a population of healthy preterm neonates at term equivalent age: a diffusion tensor imaging and probabilistic tractography study. Neuroimage. 2010; 51:783–788. [PubMed: 20206706]

Mauchly JW. Significance test for sphericity of a normal n-variate distribution. The Annals of Mathematical Statistics. 1940; 11:204–209.

Merke DP, Fields JD, Keil MF, Vaituzis AC, Chrousos GP, Giedd JN. Children with classic congenital adrenal hyperplasia have decreased amygdala volume: potential prenatal and postnatal hormonal effects. J Clin Endocrinol Metab. 2003; 88:1760–1765. [PubMed: 12679470]

Mishra A, Anderson AW, Wu X, Gore JC, Ding Z. An improved Bayesian tensor regularization and sampling algorithm to track neuronal fiber pathways in the language circuit. Med Phys. 2010; 37:4274–4287. [PubMed: 20879588]

Nordahl CW, Lange N, Li DD, Barnett LA, Lee A, Buonocore MH, Simon TJ, Rogers S, Ozonoff S, Amaral DG. Brain enlargement is associated with regression in preschool-age boys with autism spectrum disorders. Proc Natl Acad Sci USA. 2011; 108:20195–20200. [PubMed: 22123952]

Nordahl CW, Scholz R, Yang X, Buonocore MH, Simon T, Rogers S, Amaral DG. Increased rate of amygdala growth in children aged 2 to 4 years with autism spectrum disorders: a longitudinal study. Arch Gen Psychiatry. 2012; 69:53–61. [PubMed: 22213789]

Nordahl CW, Simon TJ, Zierhut C, Solomon M, Rogers SJ, Amaral DG. Brief report: methods for acquiring structural MRI data in very young children with autism without the use of sedation. J Autism Dev Disord. 2008; 38:1581–1590. [PubMed: 18157624]

Paus T, Otaky N, Caramanos Z, MacDonald D, Zijdenbos A, D'Avirro D, Gutmans D, Holmes C, Tomaiuolo F, Evans AC. In vivo morphometry of the intrasulcal gray matter in the human cingulate, paracingulate, and superior-rostral sulci: hemispheric asymmetries, gender differences and probability maps. J Comp Neurol. 1996; 376:664–673. [PubMed: 8978477]

Paus T, Zijdenbos A, Worsley K, Collins DL, Blumenthal J, Giedd JN, Rapoport JL, Evans AC. Structural maturation of neural pathways in children and adolescents: in vivo study. Science. 1999; 283:1908–1911. [PubMed: 10082463]

Peterson BS. Brain imaging studies of the anatomical and functional consequences of preterm birth for human brain development. Ann N Y Acad Sci. 2003; 1008:219–237. [PubMed: 14998887]

Pfefferbaum A, Mathalon DH, Sullivan EV, Rawles JM, Zipursky RB, Lim KO. A quantitative magnetic resonance imaging study of changes in brain morphology from infancy to late adulthood. Archives of Neurology. 1994; 51:874–887. [PubMed: 8080387]

Philippi CL, Mehta S, Grabowski T, Adolphs R, Rudrauf D. Damage to association fiber tracts impairs recognition of the facial expression of emotion. J Neurosci. 2009; 29:15089–15099. [PubMed: 19955360]

Pierpaoli C, Basser PJ. Toward a quantitative assessment of diffusion anisotropy. Magn Reson Med. 1996; 36:893–906. [PubMed: 8946355]

Powell HWR, Parker GJM, Alexander DC, Symms MR, Boulby PA, Wheeler-Kingshott CAM, Barker GJ, Noppeney U, Koepp MJ, Duncan JS. Hemispheric asymmetries in language-related pathways: A combined functional MRI and tractography study. Neuroimage. 2006; 32:388–399. [PubMed: 16632380]

Pujol J, López A, Deus J, Cardoner N, Vallejo J, Capdevila A, Paus T. Anatomical variability of the anterior cingulate gyrus and basic dimensions of human personality. Neuroimage. 2002; 15:847–855. [PubMed: 11906225]

Qiu A, Fortier MV, Bai J, Zhang X, Chong YS, Kwek K, Saw SM, Godfrey KM, Gluckman PD, Meaney MJ. Morphology and microstructure of subcortical structures at birth: a large-scale Asian neonatal neuroimaging study. Neuroimage. 2013; 65:315–323. [PubMed: 23000785]

Qiu D, Tan LH, Zhou K, Khong PL. Diffusion tensor imaging of normal white matter maturation from late childhood to young adulthood: voxel-wise evaluation of mean diffusivity, fractional anisotropy, radial and axial diffusivities, and correlation with reading development. Neuroimage. 2008; 41:223–232. [PubMed: 18395471]

Rametti G, Carrillo B, Gómez-Gil E, Junque C, Zubiarre-Elorza L, Segovia S, Gomez Á, Guillamon A. The microstructure of white matter in male to female transsexuals before cross-sex hormonal treatment. A DTI study. J Psychiatr Res. 2011; 45:949–954. [PubMed: 21195418]

Rauschecker AM, Deutsch GK, Ben-Shachar M, Schwartzman A, Perry LM, Dougherty RF. Reading impairment in a patient with missing arcuate fasciculus. Neuropsychologia. 2009; 47:180–194. [PubMed: 18775735]

Rodrigo S, Naggara O, Oppenheim C, Golestani N, Poupon C, Cointepas Y, Mangin JF, Le Bihan D, Meder JF. Human Subinsular Asymmetry Studied by Diffusion Tensor Imaging and Fiber Tracking. American Journal of Neuroradiology. 2007; 28:1526–1531. [PubMed: 17846205]

Rolheiser, T.; Stamatakis, EA.; Tyler, LK. Dynamic processing in the human language system: synergy between the arcuate fascicle and extreme capsule. 2011.

Rosenberger PB, Hier DB. Cerebral asymmetry and verbal intellectual deficits. Ann Neurol. 1980; 8:300–304. [PubMed: 7436373]

Schmithorst VJ. Developmental sex differences in the relation of neuroanatomical connectivity to intelligence. Intelligence. 2009; 37:164–173. [PubMed: 21297966]

Schmithorst VJ, Holland SK, Dardzinski BJ. Developmental differences in white matter architecture between boys and girls. Hum Brain Mapp. 2008; 29:696–710. [PubMed: 17598163]

Schneiderman JS, Buchsbaum MS, Haznedar MM, Hazlett EA, Brickman AM, Shihabuddin L, Brand JG, Torosjan Y, Newmark RE, Tang C, Aronowitz J, Paul-Odouard R, Byne W, Hof PR. Diffusion Tensor Anisotropy in Adolescents and Adults. Neuropsychobiology. 2007; 55:96–111. [PubMed: 17587876]

Scicli AP, Petrovich GD, Swanson LW, Thompson RF. Contextual Fear Conditioning Is Associated With Lateralized Expression of the Immediate Early Gene c-fos in the Central and Basolateral Amygdalar. Nuclei Behav Neurosci. 2004; 118:5–14. [PubMed: 14979778]

Sled JG, Zijdenbos AP, Evans AC. A nonparametric method for automatic correction of intensity nonuniformity in MRI data. IEEE Trans Med Imaging. 1998; 17:87–97. [PubMed: 9617910]

Smith SM. Fast robust automated brain extraction. Hum Brain Mapp. 2002; 17:143–155. [PubMed: 12391568]

Song SK, Sun SW, Ju WK, Lin SJ, Cross AH, Neufeld AH. Diffusion tensor imaging detects and differentiates axon and myelin degeneration in mouse optic nerve after retinal ischemia. Neuroimage. 2003; 20:1714–1722. [PubMed: 14642481]

Song SK, Sun SW, Ramsbottom MJ, Chang C, Russell J, Cross AH. Dysmyelination revealed through MRI as increased radial (but unchanged axial) diffusion of water. Neuroimage. 2002; 17:1429–1436. [PubMed: 12414282]

Sowell ER, Peterson BS, Kan E, Woods RP, Yoshii J, Bansal R, Xu D, Zhu H, Thompson PM, Toga AW. Sex differences in cortical thickness mapped in 176 healthy individuals between 7 and 87 years of age. Cereb Cortex. 2007; 17:1550–1560. [PubMed: 16945978]

Sun SW, Liang HF, Trinkaus K, Cross AH, Armstrong RC, Song SK. Noninvasive detection of cuprizone induced axonal damage and demyelination in the mouse corpus callosum. Magn Reson Med. 2006; 55:302–308. [PubMed: 16408263]

Thiebaut de Schotten M, Ffytche DH, Bizzi A, Dell'acqua F, Allin M, Walshe M, Murray R, Williams SC, Murphy DGM, Catani M. Atlasing location, asymmetry and inter-subject variability of white matter tracts in the human brain with MR diffusion tractography. Neuroimage. 2011; 54:49–59. [PubMed: 20682348]

Thomalla G, Glauche V, Koch MA, Beaulieu C, Weiller C, Röther J. Diffusion tensor imaging detects early Wallerian degeneration of the pyramidal tract after ischemic stroke. Neuroimage. 2004; 22:1767–1774. [PubMed: 15275932]

Trivedi R, Agarwal S, Rathore RKS, Saksena S, Tripathi RP, Malik GK, Pandey CM, Gupta RK. Understanding Development and Lateralization of Major Cerebral Fiber Bundles in Pediatric Population Through Quantitative Diffusion Tensor Tractography. Pediatric Research. 2009; 66:636–641. [PubMed: 19687778]

Tyszka JM, Readhead C, Bearer EL, Pautler RG, Jacobs RE. Statistical diffusion tensor histology reveals regional dysmyelination effects in the shiverer mouse mutant. Neuroimage. 2006; 29:1058–1065. [PubMed: 16213163]

Verhoeven JS, Sage CA, Leemans A, Van Hecke W, Callaert DE, Peeters R, De Cock P, Lagae L, Sunaert S. Construction of a stereotaxic DTI atlas with full diffusion tensor information for studying white matter maturation from childhood to adolescence using tractography-based segmentations. Hum Brain Mapp. 2009 NA–NA.

Wang F, Sun Z, Cui L, Du X, Wang X, Zhang H, Cong Z, Hong N, Zhang D. Anterior Cingulum Abnormalities in Male Patients With Schizophrenia Determined Through Diffusion Tensor Imaging. Am J Psychiatry. 2004; 161:573–575. [PubMed: 14992988]

Weinstein M, Ben-Sira L, Levy Y, Zachor DA, Itzhak EB, Artzi M, Tarrasch R, Eksteine PM, Hendler T, Bashat DB. Abnormal white matter integrity in young children with autism. Hum Brain Mapp. 2010; 32:534–543. [PubMed: 21391246]

Westerhausen R, Huster RJ, Kreuder F, Wittling W, Schweiger E. Corticospinal tract asymmetries at the level of the internal capsule: is there an association with handedness? Neuroimage. 2007; 37:379–386. [PubMed: 17601751]

Westlye LT, Walhovd KB, Dale AM, Bjørnerud A, Due-Tønnessen P, Engvig A, Grydeland H, Tamnes CK, Ostby Y, Fjell AM. Life-span changes of the human brain white matter: diffusion tensor imaging (DTI) and volumetry. Cereb Cortex. 2010; 20:2055–2068. [PubMed: 20032062]

Wilde EA, McCauley SR, Chu Z, Hunter JV, Bigler ED, Yallampalli R, Wang ZJ, Hanten G, Li X, Ramos MA, Sabir SH, Vasquez AC, Menefee D, Levin HS. Diffusion tensor imaging of hemispheric asymmetries in the developing brain. Journal of Clinical and Experimental Neuropsychology. 2009; 31:205–218. [PubMed: 19052951]

Wolff JJ, Gu H, Gerig G, Elison JT, Styner M, Gouttard S, Botteron KN, Dager SR, Dawson G, Estes AM, Evans AC, Hazlett HC, Kostopoulos P, McKinstry RC, Paterson SJ, Schultz RT, Zwaigenbaum L, Piven J. IBIS Network. Differences in white matter fiber tract development present from 6 to 24 months in infants with autism. Am J Psychiatry. 2012; 169:589–600. [PubMed: 22362397]

Wrase J, Klein S, Gruesser SM, Hermann D, Flor H, Mann K, Braus DF, Heinz A. Gender differences in the processing of standardized emotional visual stimuli in humans: a functional magnetic resonance imaging study. Neurosci Lett. 2003; 348:41–45. [PubMed: 12893421]

Yap PT, Fan Y, Chen Y, Gilmore JH, Lin W, Shen D. Development trends of white matter connectivity in the first years of life. PloS one. 2011; 6:e24678. [PubMed: 21966364]

Yeatman JD, Dougherty RF, Ben-Shachar M, Wandell BA. Development of white matter and reading skills. Proc Natl Acad Sci USA. 2012a; 109:E3045–53. [PubMed: 23045658]

Yeatman JD, Dougherty RF, Myall NJ, Wandell BA, Feldman HM. Tract profiles of white matter properties: automating fiber-tract quantification. PloS one. 2012b; 7:e49790. [PubMed: 23166771]

Yeatman JD, Dougherty RF, Rykhlevskaia E, Sherbondy AJ, Deutsch GK, Wandell BA, Ben-Shachar M. Anatomical properties of the arcuate fasciculus predict phonological and reading skills in children. J Cogn Neurosci. 2011; 23:3304–3317. [PubMed: 21568636]

Yücel M, Stuart GW, Maruff P, Velakoulis D, Crowe SF, Savage G, Pantelis C. Hemispheric and gender-related differences in the gross morphology of the anterior cingulate/paracingulate cortex in normal volunteers: an MRI morphometric study. Cereb Cortex. 2001; 11:17–25. [PubMed: 11113032]

Yücel M, Wood SJ, Phillips LJ, Stuart GW, Smith DJ, Yung A, Velakoulis D, McGorry PD, Pantelis C. Morphology of the anterior cingulate cortex in young men at ultra-high risk of developing a psychotic illness. Br J Psychiatry. 2003; 182:518–524. [PubMed: 12777343]

Zhang J, Jones M, DeBoy CA, Reich DS, Farrell JAD, Hoffman PN, Griffin JW, Sheikh KA, Miller MI, Mori S, Calabresi PA. Diffusion tensor magnetic resonance imaging of Wallerian degeneration in rat spinal cord after dorsal root axotomy. J Neurosci. 2009; 29:3160–3171. [PubMed: 19279253]

Highlights

- We used white-matter tractography in children between 2 and 5 years of age
- We examined 4 diffusion parameters at 99 locations along 18 major tracts
- Diffusion parameters varied between hemispheres and along the length of most tracts
- Sexual dimorphisms were found in several tracts
- The relationship between age and diffusion parameters varied along tract length

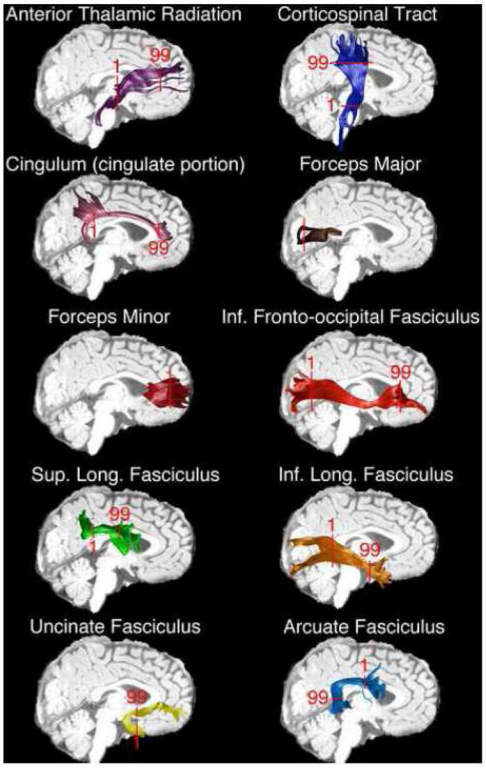

Figure 1. White-Matter Tracts Examined

AFQ tractography identifies major white matter tracts in children between 26 and 48 months. Single subject results are shown for each of the tracts used in the current analysis. In addition, red markers denoting the start (1) and termination (99) of nodal quantification are overlaid onto each tracts bundle. In the forceps major and minor quantification originated in the left hemisphere and proceeded to the right.

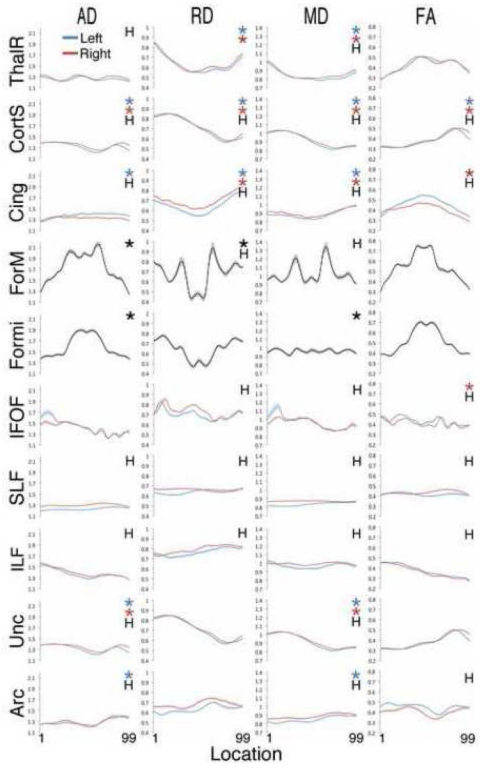

Figure 2. Diffusion Parameters Vary Along the Length of Tracts

Average diffusion parameter plots in 18 tracts from typically developing children. Each plot depicts AD, RD, MD or FA between the 1st and 99th node of each tract named at left. Tract names are abbreviated as follows: ThalR = thalamic radiations, CortS = corticospinal tracts, Cing = cingulum, ForM = forceps major, Formi = forceps minor, IFOF = inferior fronto-occipital fasciculus, SLF = superior longitudinal fasciculus, ILF = inferior longitudinal fasciculus, Unc = uncinate fasciculus, Arc = arcuate fasciculus. On each plot, “H” denotes a significant difference between the left and right hemispheres and * indicates a significant effect of location for the diffusion parameter plotted.

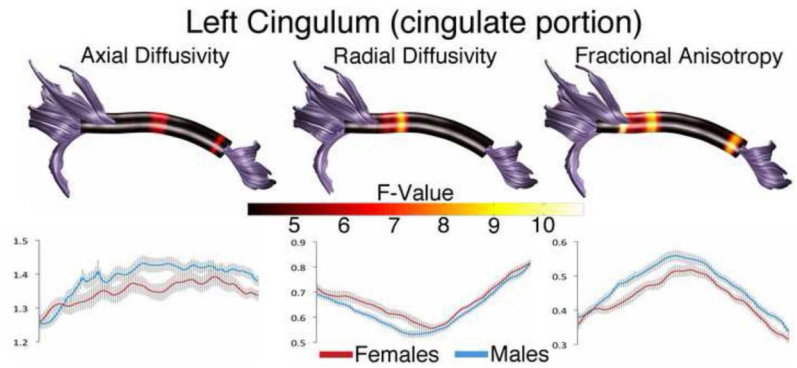

Figure 3. Sex Differences in the Left Cingulate Portion of the Cingulum

Tract profiles illustrating sex differences in AD, RD, and FA along the cingulum in typically developing male and female children. Color bar indicates F statistic values from Bonferroni-corrected analyses of covariance conducted at each location along the tract length. Significant comparisons are indicated by non-black regions. Plots for AD, RD and FA in males and females are presented below each tract profile.

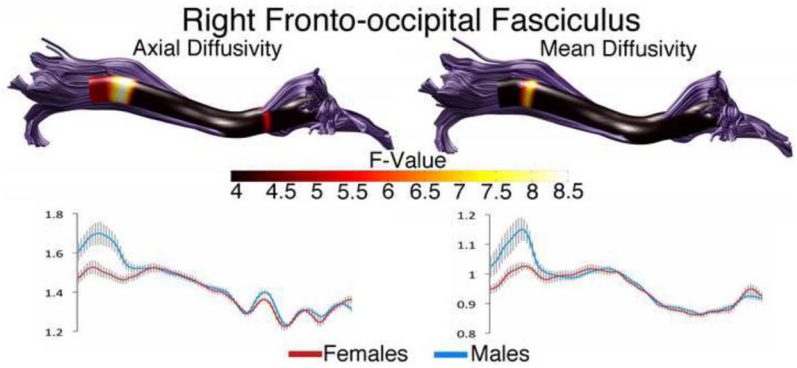

Figure 4. Sex Differences in the Right Inferior Fronto-occipital Fasciculus

Tract profiles illustrating sex differences in AD and MD along the right OFF in typically developing male and female children. Color bar indicates F statistic values from Bonferroni-corrected analyses of covariance conducted at each location along the tracts length. Significant comparisons are indicated by non-black regions. Plots for AD and MD in males and females are presented below each tract profile.

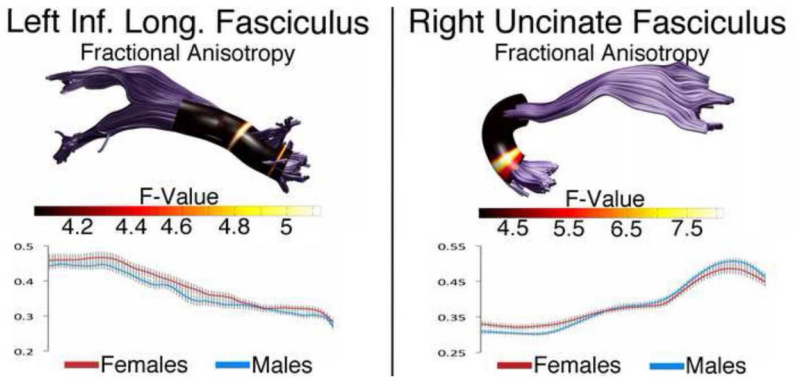

Figure 5. Sex Differences in the Left Superior Longitudinal Fasciculus and Right Uncinate Fasciculus

Tract profiles illustrating sex differences in FA along the left ILF and right uncinate in typically developing male and female children. Color bar indicates F statistic values from Bonferroni-corrected analyses of covariance conducted at each location along the tracts length. Significant comparisons are indicated by non-black regions. Corresponding plots for FA in males and females are presented below each tract profile.

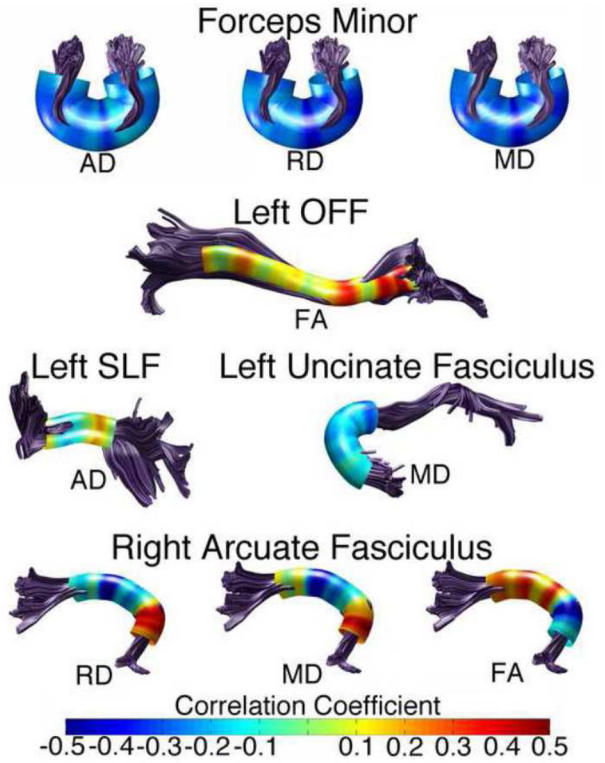

Figure 6. Relationship Between Participant Age and Diffusion Parameters in Several Tracts

Tract profiles illustrating partial correlations between age and various diffusion parameters in tracts where age emerged as a significant covariate. Scanner type and handedness are controlled. Correlation strength was variable along the tract. Colors represent the strength of the relationship as indicated by r-values. Warmer colors indicate a positive relationship and cooler colors indicate a negative one.

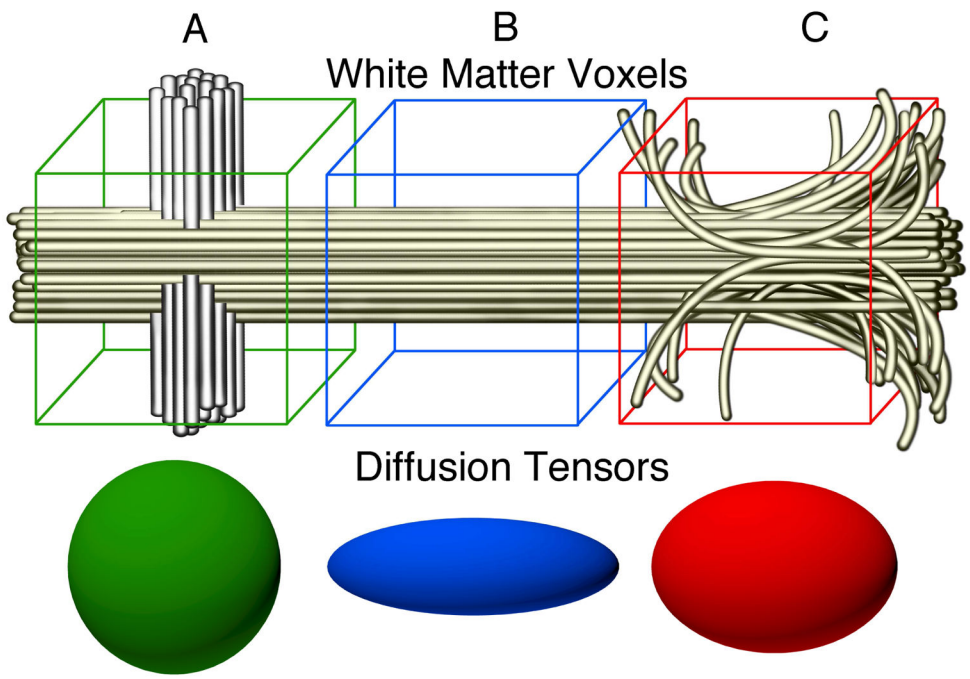

Figure 7. Environmental Contributions to Tract Anisotropy

Variations in diffusion parameters along tracts during normative development are likely a combination of tract specific (myelin content, axonal integrity) and local environment contributions. Voxel A contains a tract of interest (yellow) as well as a crossing tract (gray), resulting in low anisotropy measurements at this point. Voxel B contains only the tract of interest and exhibits high anisotropy. Within voxel C axons from nearby gray matter join the tract and some axons break off heading towards gray matter targets. The result would be a drop in anisotropy measurements at this point in the tract.

Table 1

Description of participants

Continuous Descriptors	Mean (SD)	Categorical Descriptors	N (%)
Age in months	35.28 (4.71)	Left Handed	6 (9.09)
Mullen's visual reception t-score	56.23 (11.04)	Right Handed	58 (87.88)
Mullen's receptive language t-score	52.92 (7.28)	Undetermined	2 (3.03)
Mullen's expressive language t-score	55.49 (8.73)	Caucasian	51 (77.3)
Mullen's fine-motor t-score	50 (12.68)	Asian	6 (9.1)
		African-American	3 (4.5)
		Pacific-Islander	1 (1.5)
		Other	2 (3.0)
		Not specified	3 (4.5)

Table 2

Tract Identification Rates

Tract Name	Preupgrade Scans (%)	Postupgrade Scans (%)	Total N used in Analyses
Left Thalamic Radiation	86.67	100.00	63
Right Thalamic Radiation	96.67	100.00	66
Left Corticospinal	96.67	100.00	66
Right Corticospinal	96.67	100.00	66
Left Cingulum	66.67	100.00	57
Right Cingulum	46.67	91.89	48
Forceps Major	50.00	100.00	52
Forceps Minor	100.00	100.00	67
Left Inferior Fronto-Occipital	80.00	100.00	61
Right Inferior Fronto-Occipital	83.33	100.00	62
Left Inferior Longitudinal	70.00	100.00	58
Right Inferior Longitudinal	66.67	94.59	55
Left Superior Longitudinal	93.33	97.30	64
Right Superior Longitudinal	96.67	100.00	66
Left Uncinate	93.33	100.00	65
Right Uncinate	96.67	100.00	66
Left Arcuate	80.00	91.89	58
Right Arcuate	56.67	48.65	35

Table 3

Hemisphere Differences in Tract Diffusion Properties

Tract Name	Left Hemisphere Mean (95% CI)	Right Hemisphere Mean (95% CI)	Pairwise P-value
Thalamic Radiation			
AD *	1.26 (1.25–1.27)	1.28 (1.27–1.29)	0.00
RD	0.63 (0.62–0.63)	0.63 (0.62–0.64)	0.20
MD *	0.84 (0.83–0.85)	0.85 (0.84–0.85)	0.01
FA	0.43 (0.42–0.43)	0.43 (0.42–0.44)	0.60
Corticospinal Tract			
AD *	1.42 (1.41–1.43)	1.49 (1.47–1.50)	0.00
RD *	0.55 (0.54–0.56)	0.62 (0.60–0.63)	0.00
MD *	0.84 (0.83–0.85)	0.91 (0.90–0.92)	0.00
FA *	0.55 (0.54–0.56)	0.52 (0.51–0.53)	0.00
Cingulum			
AD *	1.38 (1.35–1.40)	1.32 (1.30–1.34)	0.00
RD *	0.64 (0.62–0.65)	0.69 (0.68–0.71)	0.00
MD *	0.88 (0.87–0.90)	0.90 (0.89–0.92)	0.01
FA *	0.46 (0.45–0.47)	0.40 (0.39–0.41)	0.00
Inferior Fronto-Occipital			
AD	1.41 (1.40–1.43)	1.42 (1.40–1.44)	0.51
RD *	0.70 (0.69–0.71)	0.73 (0.72–0.74)	0.00
MD *	0.94 (0.93–0.95)	0.96 (0.95–0.97)	0.00
FA *	0.43 (0.42–0.44)	0.41 (0.40–0.42)	0.00
Superior Longitudinal			
AD *	1.23 (1.21–1.24)	1.30 (1.28–1.32)	0.00
RD *	0.64 (0.63–0.66)	0.66 (0.65–0.67)	0.01
MD *	0.84 (0.82–0.85)	0.87 (0.86–0.89)	0.00
FA *	0.42 (0.40–0.43)	0.43 (0.42–0.44)	0.01
Inferior Longitudinal			
AD *	1.37 (1.36–1.39)	1.39 (1.38–1.41)	0.02
RD *	0.75 (0.74–0.76)	0.79 (0.78–0.80)	0.00
MD *	0.96 (0.95–0.97)	0.99 (0.98–1.00)	0.00
FA *	0.39 (0.38–0.39)	0.36 (0.36–0.37)	0.00
Uncinate			
AD *	1.32 (1.30–1.33)	1.35 (1.34–1.36)	0.00
RD	0.71 (0.70–0.72)	0.72 (0.71–0.73)	0.31
MD *	0.91 (0.91–0.92)	0.93 (0.92–0.93)	0.00
FA	0.38 (0.38–0.39)	0.39 (0.38–0.40)	0.05

Tract Name	Left Hemisphere Mean (95% CI)	Right Hemisphere Mean (95% CI)	Pairwise P-value
Arcuate			
AD	1.30 (1.27–1.32)	1.29 (1.27–1.31)	0.40
RD *	0.63 (0.61–0.65)	0.68 (0.66–0.70)	0.00
MD *	0.85 (0.84–0.87)	0.88 (0.87–0.90)	0.00
FA *	0.46 (0.44–0.47)	0.41 (0.39–0.42)	0.00
Forceps Major			
AD	1.75 (1.70–1.79)	1.73 (1.68–1.77)	0.08
RD *	0.64 (0.61–0.68)	0.71 (0.66–0.75)	0.04
MD *	1.01 (0.97–1.05)	1.05 (1.00–1.09)	0.04
FA	0.57 (0.55– 0.59)	0.52 (0.50–0.54)	0.10
Forceps Minor			
AD	1.61 (1.60–1.63)	1.63 (1.61–1.64)	0.74
RD	0.66 (0.64–0.67)	0.65 (0.63–0.66)	0.34
MD	0.96 (0.96–0.99)	0.98 (0.96–0.99)	0.35
FA	0.52 (0.51–0.53)	0.53 (0.52–0.54)	0.32

* denotes a significant between hemisphere difference with $p < 0.05$

Table 4

Analysis of Variation in Diffusion Properties Along Tract Length

	Effect of Nodes			
Tract Name	**AD**	**RD**	**MD**	**FA**
Left Thalamic Radiation	F = 1.11, p = 0.36	F = 5.17, p < 0.00 *	F = 4.13, p < 0.00 *	F = 2.27, p = 0.07
Right Thalamic Radiation	F = 1.26, p = 0.28	F = 2.94, p = 0.02 *	F = 2.87, p = 0.02 *	F = 1.33, p = 0.26
Left Corticospinal	F = 3.59, p < 0.00 *	F = 10.15, p < 0.00 *	F = 10.45, p < 0.00 *	F = 3.23, p = 0.01 *
Right Corticospinal	F = 9.70, p < 0.00 *	F = 16.91, p < 0.00 *	F = 17.60, p < 0.00 *	F = 6.58, p < 0.00 *
Left Cingulum	F = 2.39, p = 0.03 *	F = 2.99, p < 0.00 *	F = 5.23, p = 0.01 *	F = 0.78, p = 0.58
Right Cingulum	F = 1.69, p = 0.12	F = 4.04, p < 0.00 *	F = 4.86, p < 0.00 *	F = 2.06, p = 0.05 *
Forceps Major	F = 2.44, p = 0.02 *	F = 1.30, p = 0.03 *	F = 1.52, p = 0.19	F = 1.63, p = 0.12
Forceps Minor	F = 2.24, p =0.04 *	F = 1.88, p = 0.10	F = 2.99, p = 0.01 *	F = 0.84, p = 0.54
Left Inferior Fronto-Occipital	F = 1.30, p = 0.26	F = 0.30, p = 0.88	F = 0.52, p = 0.66	F = 0.99, p = 0.44
Right Inferior Fronto-Occipital	F = 1.85, p = 0.14	F = 1.94, p = 0.13	F = 1.86, p = 0.15	F = 2.34, p = 0.02 *
Left Superior Longitudinal	F = 0.63, p = 0.61	F = 1.18, p = 0.32	F = 1.32, p = 0.27	F = 0.75, p = 0.52
Right Superior Longitudinal	F = 0.71, p = 0.55	F = 2.29, p = 0.08	F = 2.35, p = 0.08	F = 0.63, p = 0.39
Left Inferior Longitudinal	F = 0.63, p = 0.63	F = 1.09, p = 0.37	F = 0.71, p = 0.59	F = 1.45, p = 0.21
Right Inferior Longitudinal	F = 1.54, p = 0.19	F = 0.86, p = 0.50	F = 0.97, p = 0.42	F = 1.97, p = 0.06
Left Uncinate	F = 4.46, p < 0.00 *	F = 1.13, p = 0.34	F = 3.77, p < 0.00 *	F = 1.50, p = 0.19
Right Uncinate	F = 3.00, p = 0.02 *	F = 2.04, p = 0.08	F = 3.62, p = 0.01 *	F = 1.08, p = 0.37
Left Arcuate	F = 3.56, p < 0.00 *	F = 0.95, p = 0.44	F = 3.40, p = 0.01 *	F = 0.78, p = 0.57
Right Arcuate	F = 1.12, p = 0.35	F = 1.26, p = 0.28	F = 2.19, p = 0.05	F = 0.99, p = 0.43

* denotes a significant between nodes difference with $p < 0.05$